RSC Advances

PAPER

View Article Online
View Journal | View Issue

Cite this: *RSC Adv.*, 2017, **7**, 4291

Systematic analysis of structural and topological properties: new insights into $PuO_2(H_2O)_n^{2+}$ ($n = 1–6$) complexes in the gas phase

Peng Li,*[a] Wenxia Niu*[b] and Tao Gao[c]

Received 21st November 2016
Accepted 29th December 2016

DOI: 10.1039/c6ra27087e

www.rsc.org/advances

The equilibrium structure, stabilities, electronic structures, chemical bonding and topological properties of $PuO_2(H_2O)_n^{2+}$ ($n = 1–6$) complexes in the gas phase have been systematically investigated by different levels of theory. The results indicate that all the ground states of these complexes are triplet. The five water molecules of $PuO_2(H_2O)_m^{2+}$ ($m = 1–5$) are arranged on the equatorial plane of plutonyl. Reactivity analysis of $PuO_2(H_2O)_5^{2+}$ shows that the oxygen atom of the sixth water molecule is connected by hydrogen-bonds to the two water molecules which are on the equatorial plane of $PuO_2(H_2O)_5^{2+}$. The optimized geometries are in agreement with available theoretical and experimental results. The weak covalent interactions of Pu–ligand bonds were evaluated by the electron localization function and atoms in molecules analyses. The orbital interactions were investigated by analysis of total, partial, and overlap population density of state diagrams. Besides, a reduced density gradient approach was implemented to analyze the weak interactions and steric repulsions present in $PuO_2(H_2O)_5^{2+}$ and $PuO_2(H_2O)_6^{2+}$ complexes.

1 Introduction

The chemistry of dipositive actinyl ions, particularly plutonyl complexes, is of major importance in nuclear waste reprocessing cycles and safe storage.[1–6] It is worth mentioning that Pu ions have a higher-valence above +4 (*e.g.*, +5, +6, and +7), and can easily form a variety of complexes with other ligands. Another interesting topic of this area is the active effects of the 5f electrons, due to the f elements having a high oxophilicity feature.[7] Therefore, the interactions of plutonyl with other ligand molecules have attracted considerable attention.[8–18] In particular, researches have focused on the interaction of plutonyl with H_2O molecules, which is a major issue in secure nuclear storage, because H_2O plays a catalytic role in plutonium corrosion.[19,20]

Theoretical research in this area is more common than experimental; this may be due to the high activity and radioactivity which causes difficulties for experimental studies. In a recent experimental study,[11] the hydration and oxidation of gas-phase plutonyl monovalent ions were investigated by electrospray ionization mass spectrometry (ESI-MS), and the ESI mass spectra of $PuO_2(H_2O)_n^+$ ($n = 0–5$) were obtained. In contrast, tremendous theoretical works have been performed to exploring the properties of $PuO_2(H_2O)_n^{2+}$ complexes.[10,12,16,17,21–24] Cao *et al.* have utilized density functional theory (DFT) methods to investigate the structural properties and vibrational frequencies of $PuO_2(H_2O)_m^{2+}$ complexes ($m = 4–6$).[10] Most of the previous studies predicted that plutonyl(VI) ions will be the favorable structure, therefore, the equilibrium structure of $PuO_2(H_2O)_5^{2+}$ has been well studied.[12,16,17,20–23] On the other hand, these theoretical studies significantly suggest that DFT is an appropriate and successful method to access the nature of $PuO_2(H_2O)_n^{2+}$ complexes.

As seen from the above survey of $PuO_2(H_2O)_n^{2+}$ complexes, there are uncertainties of the bonds characterization, bonding mechanism and the effect of plutonyl orbitals in the interaction. Therefore, detailed interaction mechanisms and the topological properties as well as orbitals information need to be systematically examined.

The main focus of the present work is to perform a new thorough investigation of the $PuO_2(H_2O)_n^{2+}$ complexes ($n = 1–6$). The optimized geometries and electronic state properties of these complexes are reported. The covalent interactions were evaluated for Pu–ligand bonds in these complexes with electron localization function (ELF) and atoms in molecules (AIM) analyses. The roles of plutonyl orbitals were analyzed by total and partial density of state (TDOS and PDOS), and overlap population density of state (OPDOS) analysis. In addition, the weak interactions and steric repulsions exist in these complexes were studied by reduced density gradient (RDG) approach.

2 Computational details

Geometry optimization and frequency calculation of the stable structures were performed at the B3LYP,[25,26] B3PW91,[27] PBE0 (ref.

[a]College of Physics and Electronic Engineering, Shanxi University, Taiyuan, 030006, China. E-mail: lip@sxu.edu.cn
[b]Department of Physics, Taiyuan Normal University, Taiyuan, 030031, China. E-mail: nwx_ky@163.com
[c]Institute of Atomic and Molecular Physics, Sichuan University, Chengdu, 610065, China

28) and PW91PW91 (ref. 29) methods, along with Stuttgart–Dresden–Bonn relativistic effective core potential (RECP)[30] for Pu atom. This small core RECP, named as SDD, replaces 60 electrons in inner shells,[1–4] leaving the 5s, 5p, 5d, 5f, 6s, 6p, 6d and 7s shells as the valence electrons. For O and H atoms, the 6-311++G(d,p) basis sets by Pople and coworkers were employed.[31] Calculations were carried out by using the Gaussian 03 programs.[32] The geometry structures of these complexes were identified to be one minimum in potential energy, and their stability were examined by molecular dynamics. The current computational scheme has been successfully performed in actinide systems.[6,33–40] Specifically, previous works show that B3LYP/SDD and PW91/SDD methods have good performance in the structure and frequencies computation for Pu–H_2O system.[6]

With the aim of deeply investigate the nature of the bonding, a systematic topological description of these complexes was performed. The wavefunction files (.wfn) which obtained from geometry optimization and frequency calculation were used as input files of the Multiwfn[41] package to perform the ELF[42,43] and AIM[44] analysis. In order to gathering insights about the participation of plutonyl orbitals in the chemical bonds of complexes, TDOS, PDOS, and OPDOS[45,46] analysis were also performed. In addition, the reduced density gradient proposed by Yang *et al.*[47] was used to obtain a deep insight into the weak interactions and steric repulsions in titled complexes.

3 Results and discussion

To evaluate the accuracy of current computational schemes for plutonyl systems, first, we calculated the bond distances and vibrational frequencies of PuO, PuO_2 and PuO_2^{2+} molecule. The results are listed in Table 1 along with the corresponding available experimental values and previous theoretical results. As can be seen, our results are in agreement with available experimental values, and have good consistency with other theoretical results.

Table 1 Bond distances (Å) and vibrational frequencies (cm^{-1}) of PuO, PuO_2 and PuO_2^{2+} in the gas phase at the different level of theories

Methods	Methods	r(Pu–O)	Vibrational frequencies
PuO	B3LYP/SDD[a]	1.832	792.73
	B3PW91/SDD[a]	1.817	814.97
	PBE0/SDD[a]	1.813	816.41
	PW91/SDD[a]	1.832	768.92
	CASPT2[b]	1.818	
	PW91/SDD[c]	1.828	
	Expt.[d]		822.28 (Ar), 817.27 (Kr)
PuO_2	B3LYP/SDD[a]	1.816	808.41, 757.01, 160.11
	B3PW91/SDD[a]	1.801	833.03, 778.24, 170.32
	PBE0/SDD[a]	1.794	844.90, 789.74, 173.52
	PW91/SDD[a]	1.804	823.57, 709.59, 173.61
	M06/SDD[c]	1.786	
	PW91/SDD[c]	1.802	
	Expt.[d]		794.2 (Ar), 786.8 (Kr)
PuO_2^{2+}	B3LYP/SDD[a]	1.673	1101.36, 237.98, 250.20, 980.20
	B3PW91/SDD[a]	1.662	1127.62, 244.23, 255.84, 1010.96
	PBE0/SDD[a]	1.653	1153.99, 257.02, 263.77, 1041.14
	PW91/SDD[a]	1.695	1039.55, 207.96, 210.55, 915.67
	B3LYP/RECP78[e]	1.663	
	MP2/RECP78[e]	1.686	
	Expt.	1.74[f]	1043, 218 × 2, 1020[g]

[a] This work, SDD for Pu and 6-311++G(d,p) for O atoms. [b] Ref. 48. [c] Ref. 49. [d] Ref. 50. [e] Ref. 10. [f] Ref. 51. [g] Ref. 52.

3.1 Geometric structures and electronic properties

In order to obtain minimum energy structures, dozens of possible structures of $PuO_2(H_2O)_n^{2+}$ complexes (n = 1–6) were constructed, and taking into account different possible spin states. Geometry optimization was performed without symmetry constrain, and their corresponding ground state geometries in the gas phase were located. Moreover, the stability of these stable structures was confirmed by Born–Oppenheimer molecular dynamics (BOMD)[53] simulations at 300 K. Geometric parameters are reported in Fig. 1 for different levels of theory.

As can been seen from Fig. 1, the optimized geometries show little dependence on the level of theory. Our results indicate that the ground electronic state of these complexes are triplet. In terms of geometry, we can see that water molecules of $PuO_2(H_2O)_m^{2+}$ (m = 1–5) are arranged on the equatorial plane of the plutonyl group. In particular, water molecules wherein $PuO_2(H_2O)_3^{2+}$ and $PuO_2(H_2O)_4^{2+}$ are almost in the equivalent position.

To evaluate the sites of six water molecules in $PuO_2(H_2O)_6^{2+}$, we performed the reactivity analysis by using electrostatic potential (ESP) on molecular vdW surface of $PuO_2(H_2O)_5^{2+}$. ESP on vdW surface has been proved as a critical for studying intermolecular interaction, and widely used for prediction of nucleophilic and electrophilic sites. More negative ESP signifies this region has the stronger ability to attract electrophiles, on the contrary, more positive ESP site has the stronger ability to attract nucleophiles.[54] The ESP-mapped vdW surface of $PuO_2(H_2O)_5^{2+}$ is shown in Fig. 2. It can be seen that, the surface maximum of ESP present at the H atoms of water molecule. Therefore, from ESP point of view, these H atoms of the $PuO_2(H_2O)_5^{2+}$ are the primary bonding site of O atom. After optimization, as seen from Fig. 1, we found that the oxygen atom of sixth water molecule is connected to the two water molecules which on the equatorial plane of $PuO_2(H_2O)_5^{2+}$ by hydrogen-bonds.

In terms of bond length, with the increase of water molecules, the bond length of Pu–O_{yl} and Pu=O increased slightly. Taking the calculation result of B_3LYP/SDD as an example, for bond length of Pu–O_{yl}, 2.293 Å for $PuO_2(H_2O)^{2+}$ and 2.469 Å for $PuO_2(H_2O)_6^{2+}$; for bond length of Pu=O, 1.673 Å for $PuO_2(H_2O)^{2+}$ and 1.705 Å for $PuO_2(H_2O)_6^{2+}$, respectively.

3.2 Bonding features

The bonding nature of Pu–O for these complexes have been investigated using ELF and AIM analytical method. It is worth mentioned that ELF and AIM are appropriate and successful tools to analyzing bonding mechanism and have been applied in many actinides complexes investigations. In addition, ELF

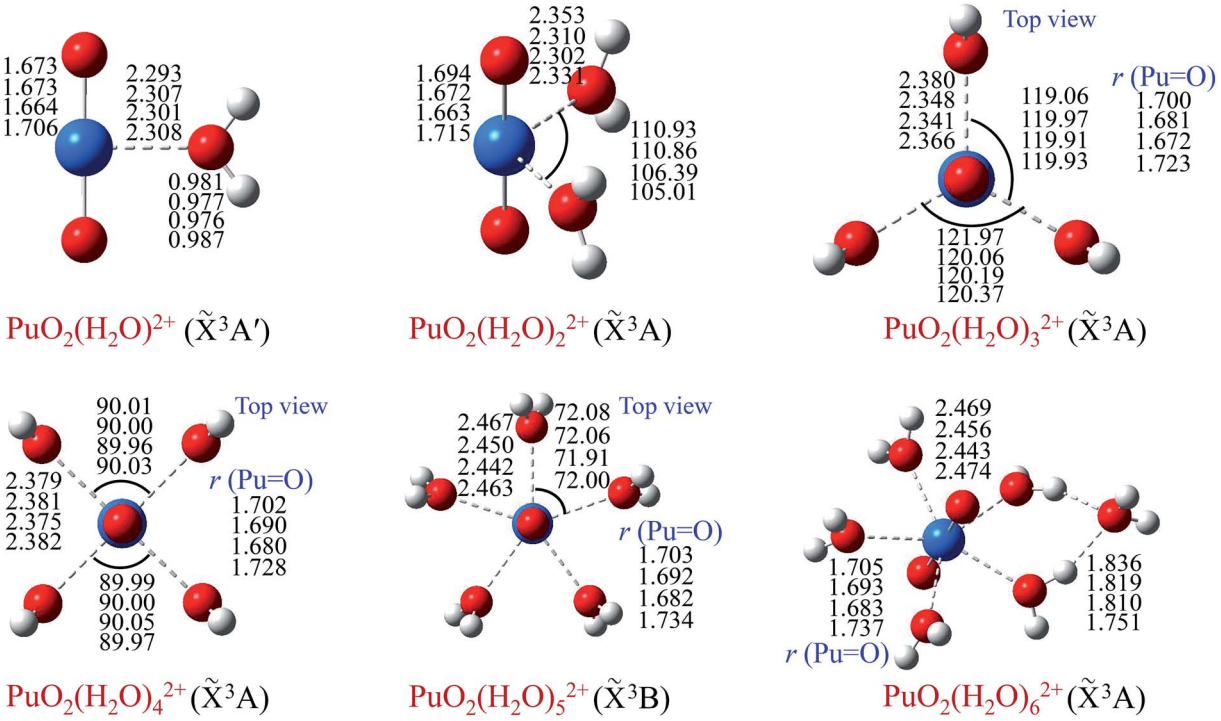

Fig. 1 Structures and selected geometric parameters of $PuO_2(H_2O)_n^{2+}$ complexes ($n = 1$–6), which were optimized at the B3LYP/SDD, B3PW91/SDD, PBE0/SDD and PW91/SDD levels of theory (from top to bottom rows, respectively). r(Pu=O) represents the bond length of plutonyl. Bond distances are in Å, and angles are in degrees.

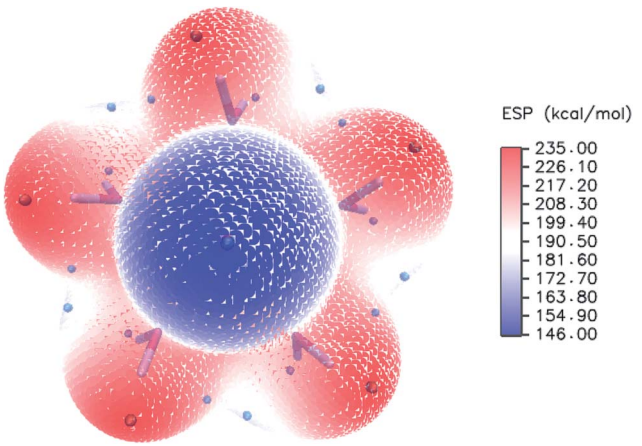

Fig. 2 ESP-mapped molecular vdW surface of $PuO_2(H_2O)_5^{2+}$. The unit is in kcal mol^{-1}. Surface local minima and maxima of ESP are represented as green and orange spheres, respectively.

obtained from small-core RECP has been proven to correctly analyze the topological properties.[55,56]

The ELF shaded-surface-projection map of the titled complexes are displayed in Fig. 3. As can be seen, these are disynaptic valence basins between the Pu and O_{yl} atoms, which indicate that there are covalent bonds formation between plutonyl and H_2O molecules.

In order to further exploring the chemical-bonding natures of these complexes, we employ a more quantitative method, the atoms in molecules (AIM) analysis. The different topological properties including electron density $\rho(r)$ and its Laplacian $\nabla^2\rho(r)$, kinetic electron energy density $G(r)$, potential energy density $V(r)$ and the total energy density $H(r)$ of the (3, −1) bond critical points (BCP) were calculated. The corresponding results are shown in Table 2.

As the criterion proposed by Cremer and Kraka:[57] $|V(r)| > G(r)$, $H(r)$ is negative, corresponds to covalent interactions; conversely, for closed-shell interactions, $|V(r)| < G(r)$, $H(r)$ is positive. This criterion was proved to be very sufficient to explore the bonding characteristics for actinide system.[37–39] As shown in Table 2, the $H(r)$ values of all calculated BCPs in the $PuO_2(H_2O)_n^{2+}$ are negative,

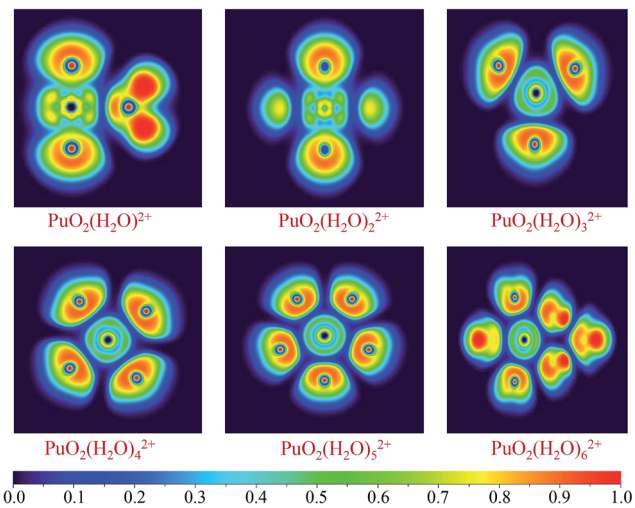

Fig. 3 Two-dimensional filled-color diagrams of ELF ($\eta = 0.70$) at the B3PW91/SDD level of theory.

Table 2 Topological properties of the electron density calculated at the (3, −1) BCPs of $PuO_2(H_2O)_n^{2+}$ complexes ($n = 1$–6)

Complexes	Species	$\rho(r)$	$\nabla^2\rho(r)$	$G(r)$	$V(r)$	$H(r)$
$PuO_2H_2O^{2+}$	Pu–O	0.388	0.211	0.476	−0.900	−0.424
	Pu–O_{yl}	0.074	0.314	0.085	−0.093	−0.008
$PuO_2(H_2O)_2^{2+}$	Pu–O	0.384	0.187	0.466	−0.885	−0.419
	Pu–O_{yl}	0.072	0.302	0.081	−0.087	−0.006
$PuO_2(H_2O)_3^{2+}$	Pu–O	0.375	0.191	0.448	−0.849	−0.401
	Pu–O_{yl}	0.065	0.280	0.074	−0.077	−0.003
$PuO_2(H_2O)_4^{2+}$	Pu–O	0.366	0.199	0.432	−0.815	−0.383
	Pu–O_{yl}	0.060	0.257	0.066	−0.068	−0.002
$PuO_2(H_2O)_5^{2+}$	Pu–O	0.364	0.200	0.428	−0.806	−0.378
	Pu–O_{yl}	0.051	0.215	0.054	−0.0543	−0.0003
$PuO_2(H_2O)_6^{2+}$	Pu–O	0.323	0.326	0.377	−0.673	−0.296
	Pu–O_{yl}	0.049	0.203	0.0511	−0.0513	−0.0002
	Pu–O_{yl}[a]	0.054	0.212	0.054	−0.056	−0.002
	H–O[b]	0.039	0.121	0.032	−0.034	−0.002

[a] Two special water molecules of $PuO_2(H_2O)_5^{2+}$, which connected with the sixth water molecule. [b] Hydrogen-bonds.

the corresponding $|V(r)|/G(r)$ ratio exceeds 1.0. The $H(r)$ values of Pu–O_{yl} bonds are relatively small (around −0.003), and with the increase of water molecules, this value is decreasing. These quantities suggest that the Pu–O_{yl} bonds belong to weak covalent interaction. This conclusion is consistent with the ELF analysis. In term of the connection of sixth water molecule, there are two (3, −1) BCPs between the oxygen atom of sixth water molecule and two water molecules in the vertical plane of $PuO_2(H_2O)_5^{2+}$. The corresponding $\rho(r) = 0.039$, $H(r) = -0.002$, indicating that these two bonds are hydrogen bonds.

3.3 Orbital interactions

As can be seen from the above discussion, on the basis of $PuO_2(H_2O)_5^{2+}$ complex, the additional water molecules will no longer bonding with the main PuO_2^{2+} molecule directly. To get more in-depth information about the roles that plutonyl orbitals play in the formation of plutonyl–water complexes, the TDOS, PDOS and OPDOS of $PuO_2(H_2O)_5^{2+}$ and $PuO_2(H_2O)_6^{2+}$ were calculated and plotted with Gaussian curves, the corresponding full width at half maximum (FWHM) is 0.05 a.u. The TDOS, PDOS and OPDOS graphics are depicted in Fig. 4. The vertical dashed line indicates the position of the HOMO level. Fragment 1 is defined as the plutonyl orbitals and fragment 2 is defined as the oxygen and hydrogen atom orbitals.

As seen in Fig. 4, at the position of the HOMO level, the H_2O orbitals approached the TDOS line, which means that most of the contributions to the HOMO came from the H_2O orbitals. The OPDOS values of plutonyl and H_2O orbitals are almost zero, which means that there are weak covalent characters in $PuO_2(H_2O)_5^{2+}$ and $PuO_2(H_2O)_6^{2+}$ complex. Comparing the two subgraphs, we found that the addition of the sixth water molecule had little effect on the overall DOS.

3.4 Weak interactions

With the aim of investigating the weak interactions of the $PuO_2(H_2O)_5^{2+}$ and $PuO_2(H_2O)_6^{2+}$ complexes, we performed

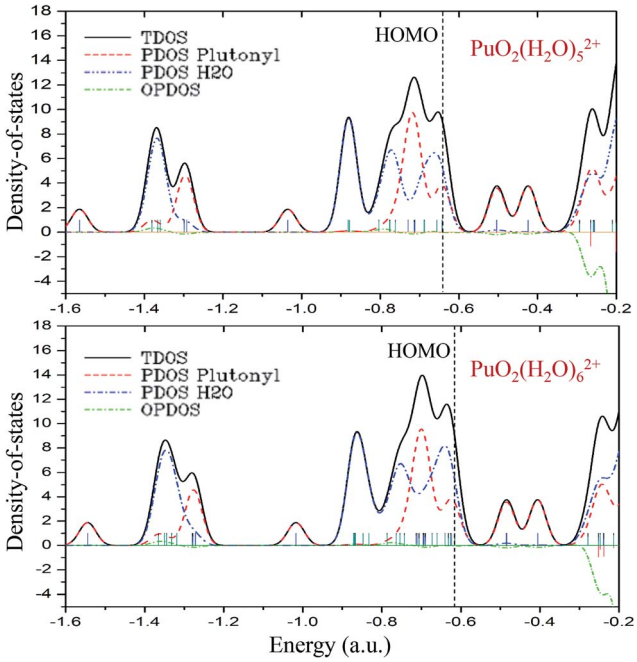

Fig. 4 The TDOS, PDOS, and OPDOS curves of $PuO_2(H_2O)_5^{2+}$ and $PuO_2(H_2O)_6^{2+}$ at the B3PW91/SDD levels of theory.

reduced density gradient (RDG) analysis. The RDG was defined as follows:[46]

$$s(r) = \frac{1}{2(3\pi^2)^{1/3}} \frac{|\nabla\rho(r)|}{\rho(r)^{4/3}}$$

where $\rho(r)$ is electron density. The RDG $s(r)$ isosurfaces are mapped with values of $\rho(r)\cdot\mathrm{sgn}(\lambda_2)$, where sgn is the signum function, and λ_2 is the sign of the second eigenvalue of the Hessian of the $\rho(r)$.

Fig. 5 shows the 3D isosurfaces ($s = 0.5$) and scatter plots of the RDG *vs.* $\rho(r)\mathrm{sign}(\lambda_2)$ were generated for $PuO_2(H_2O)_5^{2+}$ and $PuO_2(H_2O)_6^{2+}$ complexes. From the isosurfaces, we can see that the Pu–O_{yl} interaction in $PuO_2(H_2O)_6^{2+}$ is slightly weaker than that in the $PuO_2(H_2O)_5^{2+}$. The $\rho(r)\cdot\mathrm{sgn}(\lambda_2)$ value of Pu–O_{yl} interaction in the $PuO_2(H_2O)_5^{2+}$ is −0.0335 a.u., and the corresponding value in $PuO_2(H_2O)_6^{2+}$ is −0.034 a.u. In addition, there are two spikes in RDG *vs.* $\rho(r)\mathrm{sign}(\lambda_2)$ of $PuO_2(H_2O)_5^{2+}$, one is around −0.01 a.u. corresponding the van der Waals interaction between the adjacent water molecules; the other one is around 0.01 a.u., represents the steric repulsion effects between Pu and H_2O molecules which on both sides of Pu–O_{yl}. Differently, the RDG *vs.* $\rho(r)\mathrm{sign}(\lambda_2)$ of $PuO_2(H_2O)_6^{2+}$ is one more spike than that of $PuO_2(H_2O)_5^{2+}$ in the region of 0 to −0.4 a.u. This spike around −0.034 is corresponds to the hydrogen-bond interaction of the sixth H_2O molecule and two water molecules in the vertical plane of $PuO_2(H_2O)_5^{2+}$.

In order to quantitatively gauge the bond strengths, in Table 3, we computed bond dissociation energies (BDE) of Pu–O_{yl} bond for $PuO_2(H_2O)_3^{2+}$, $PuO_2(H_2O)_4^{2+}$ and $PuO_2(H_2O)_5^{2+}$ as well as hydrogen-bond for $PuO_2(H_2O)_6^{2+}$ complexes. It can be clearly seen that, as the H_2O number increases, the BDE of Pu–O_{yl} bond decrease. Taking PW91/SDD results as an example, the

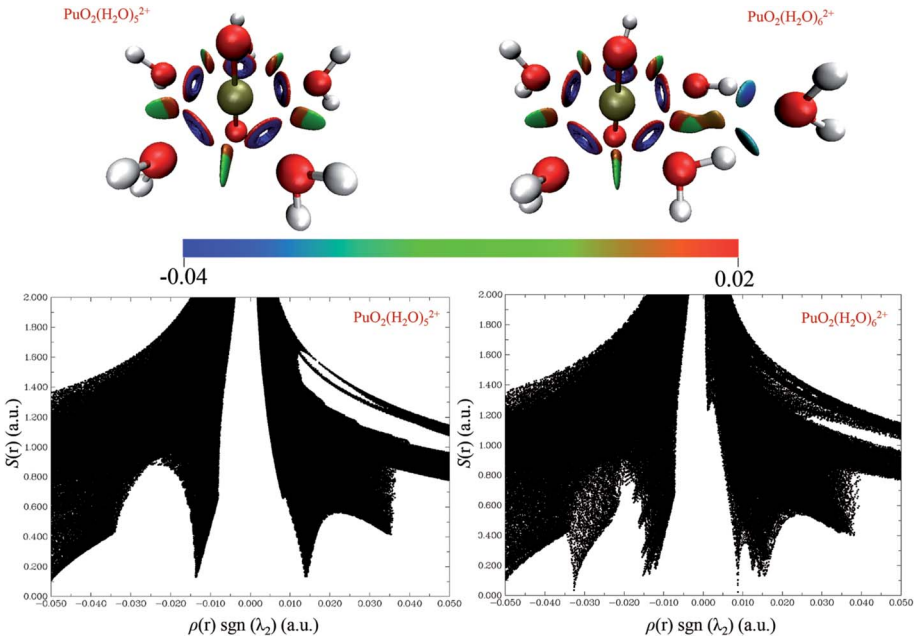

Fig. 5 3D isosurfaces ($s = 0.5$) and scatter plots of the RDG *vs.* $\rho(r)\mathrm{sign}(\lambda_2)$ were generated for $PuO_2(H_2O)_5^{2+}$ and $PuO_2(H_2O)_6^{2+}$ complexes.

Table 3 Bond dissociation energies (BDE in kcal mol^{-1}) and bond lengths (in Å) of the selected bond for $PuO_2(H_2O)_x^{2+}$ ($x = 3$–6)

Complex		B3LYP/SDD	B3PW91/SDD	PBE0/SDD	PW91/SDD
$PuO_2(H_2O)_3^{2+}$	r(Pu–O_{yl})	2.351	2.310	2.302	2.331
	BDE	42.586	49.903	45.973	49.788
$PuO_2(H_2O)_4^{2+}$	r(Pu–O_{yl})	2.379	2.381	2.375	2.382
	BDE	40.330	39.143	40.941	36.675
$PuO_2(H_2O)_5^{2+}$	r(Pu–O_{yl})	2.467	2.450	2.442	2.463
	BDE	21.150	20.413	22.967	27.145
$PuO_2(H_2O)_6^{2+}$	r(O_{6yl}–H′)	1.836	1.819	1.810	1.751
	BDE	11.133	10.794	11.637	12.287

BDE of Pu–O_{yl} for $PuO_2(H_2O)_3^{2+}$ as much as 49.788 kcal mol^{-1}, which is larger than that computed for the $PuO_2(H_2O)_4^{2+}$ (36.675 kcal mol^{-1}) and more larger than that for the $PuO_2(H_2O)_5^{2+}$ (27.145 kcal mol^{-1}). In the case of O–H hydrogen-bond for $PuO_2(H_2O)_6^{2+}$, by contrast, the BDE is smaller (12.287 kcal mol^{-1} in PW91/SDD method).

4 Conclusions

The equilibrium structure, stabilities, electronic structures, chemical bonding and topological properties of $PuO_2(H_2O)_n^{2+}$ (n = 1–6) complexes in gas phase have been systematically investigated by different levels of theory. The following conclusions were refined from the present results.

(1) The ground state geometry of these complexes was found, and our results show that all the ground states of these complexes are triplet. The water molecules of $PuO_2(H_2O)_m^{2+}$ (m = 1–5) are arranged on the equatorial plane of plutonyl. Reactivity analysis and optimization results of $PuO_2(H_2O)_6^{2+}$ show that, the oxygen atom of sixth water molecule connected with two water molecules in the vertical plane of $PuO_2(H_2O)_5^{2+}$ by hydrogen-bonds. These optimized geometries are in agreement with available theoretical and experimental results.

(2) The properties of the chemical-bonding of these complexes were evaluated with ELF, AIM and TDOS, PDOS and OPDOS analyses. The ELF and AIM analyses indicate the Pu–O_{yl} bonds have weak covalent interaction. This conclusion is consistent with the OPDOS analysis. The TDOS results show that most of the contributions to the HOMO of $PuO_2(H_2O)_5^{2+}$ and $PuO_2(H_2O)_6^{2+}$ came from the H_2O orbitals.

(3) The RDG approach was implemented to analyze the weak interactions and steric repulsions existed in $PuO_2(H_2O)_5^{2+}$ and $PuO_2(H_2O)_6^{2+}$ complexes. In addition to explaining weak covalent interactions of Pu–O_{yl}, the RDG results also suggest that the interactions of the sixth H_2O molecule and two water molecules in the vertical plane of $PuO_2(H_2O)_5^{2+}$ are hydrogen-bonds.

Acknowledgements

This work is supported by National Natural Science Foundation of China (NSFC) (Grant No. 11604187 and No. 11647040). We are very grateful to Dr Sobereva for many helpful discussions

and providing us with the Multiwfn package. We would like to thank the reviewers for the valuable suggestions on improving our paper.

References

1 R. G. Denning, *J. Phys. Chem. A*, 2007, **111**, 4125.
2 U. Wahlgren, H. Moll, I. Grenthe, B. Schimmelpfennig, L. Maron, V. Vallet and O. Gropen, *J. Phys. Chem. A*, 1999, **103**, 8257.
3 J. M. Haschke, T. H. Allen and J. L. Stakebake, *J. Alloys Compd.*, 1996, **243**, 23.
4 J. M. Haschke, T. H. Allen and L. A. Morales, *Science*, 2000, **287**, 285.
5 J. M. Haschke, T. H. Allen and L. A. Morales, *J. Alloys Compd.*, 2001, **314**, 78.
6 P. Li, W. X. Niu, T. Gao and H. Y. Wang, *ChemPhysChem*, 2014, **15**, 3078.
7 H. H. Cornehl, R. Wesendrup, M. Diefenbach and H. Schwarz, *Chem.–Eur. J.*, 1997, **3**, 1083.
8 C. Madic, G. M. Begun, D. E. Hobart and R. L. Hahn, *Inorg. Chem.*, 1984, **23**, 1914.
9 S. D. Conradson, K. D. Abney, B. D. Begg, E. D. Brady, D. L. Clark, C. den Auwer, M. Ding, P. K. Dorhout, F. J. Espinosa-Faller and P. L. Gordon, *Inorg. Chem.*, 2004, **43**, 116.
10 Z. Cao and K. Balasubramanian, *J. Chem. Phys.*, 2005, **123**, 114309.
11 D. Rios, M. C. Michelini, A. F. Lucena, J. Marcalo, T. H. Bray and J. K. Gibson, *Inorg. Chem.*, 2012, **51**, 6603.
12 K. A. Maerzke, G. S. Goff, W. H. Runde, W. F. Schneider and E. J. Maginn, *J. Phys. Chem. B*, 2013, **117**, 10852.
13 J. P. Austin, M. Sundararajan, M. A. Vincent and I. H. Hillier, *Dalton Trans.*, 2009, 5902.
14 L. H. Jones and R. A. Penneman, *J. Chem. Phys.*, 1953, **21**, 542.
15 G. A. Shamov and G. Schreckenbach, *J. Phys. Chem. A*, 2006, **110**, 12072.
16 A. Kovács, R. J. M. Konings, J. K. Gibson, I. Infante and L. Gagliardi, *Chem. Rev.*, 2015, **115**, 1725.
17 S. E. Horowitz and J. B. Marston, *J. Chem. Phys.*, 2011, **134**, 064510.
18 J. G. Du, X. Y. Sun and G. Jiang, *Int. J. Mol. Sci.*, 2016, **17**, 414.
19 J. M. Haschke, *J. Alloys Compd.*, 1998, **278**, 149.
20 J. M. Haschke, T. H. Allen and L. A. Morales, *Los Alamos Sci.*, 2000, **26**, 252.
21 P. J. Hay, R. L. Martin and G. Schreckenbach, *J. Phys. Chem. A*, 2000, **104**, 6259.
22 G. A. Shamov and G. Schreckenbach, *J. Phys. Chem. A*, 2005, **109**, 10961.
23 V. Vallet, P. Macak, U. Wahlgren and I. Grenthe, *Theor. Chem. Acc.*, 2006, **115**, 145.
24 G. Schreckenbach and G. A. Shamov, *Acc. Chem. Res.*, 2010, **43**, 19.
25 C. Lee, W. Yang and R. G. Parr, *Phys. Rev. B: Condens. Matter Mater. Phys.*, 1988, **37**, 785.
26 A. D Becke, *J. Chem. Phys.*, 1993, **98**, 5648.
27 A. D. Becke, *Phys. Rev. A*, 1998, **38**, 3098.
28 C. Adamo and V. Barone, *J. Chem. Phys.*, 1999, **110**, 6158.
29 J. P. Perdew, K. Burke and Y. Wang, *Phys. Rev. B: Condens. Matter Mater. Phys.*, 1996, **54**, 16533.
30 W. Kuchle, M. Dolg, H. Stoll and H. Preuss, *J. Chem. Phys.*, 1994, **100**, 7535.
31 R. Krishnan, J. S. Binkley, R. Seeger and J. A. Pople, *J. Chem. Phys.*, 1980, **72**, 650.
32 M. J. Frisch, G. W. Trucks, H. B. Schlegel, G. E. Scuseria, M. A. Robb and J. R. Cheeseman, *et al.*, *Gaussian 03, Revision E.01.*, Gaussian, Inc., Wallingford, CT, USA, 2004.
33 M. C. Michelini, N. Russo and E. Sicilia, *Angew. Chem., Int. Ed.*, 2006, **45**, 1095.
34 M. E. Alikhani, M. C. Michelini, N. Russo and B. Silvi, *J. Phys. Chem. A*, 2008, **112**, 12966.
35 J. Zhou and H. B. Schlegel, *J. Phys. Chem. A*, 2010, **114**, 8613.
36 K. J. De Almeida and H. A. Duarte, *Organometallics*, 2010, **29**, 3735.
37 X. F. Wang, L. Andrews and C. J. Marsden, *Chem.–Eur. J.*, 2007, **13**, 5601.
38 P. Li, W. X. Niu and T. Gao, *RSC Adv.*, 2014, **4**, 29806.
39 P. Li, W. X. Niu and T. Gao, *J. Radioanal. Nucl. Chem.*, 2015, **304**, 489.
40 P. Li, W. X. Niu and T. Gao, *J. Mol. Model.*, 2015, **21**, 316.
41 T. Lu and F. Chen, *J. Comput. Chem.*, 2012, **33**, 580.
42 A. D. Becke and K. E. Edgecombe, *J. Chem. Phys.*, 1990, **92**, 5397.
43 A. Savin, R. Nesper, S. Wengert and T. R. Fassler, *Angew. Chem., Int. Ed. Engl.*, 1997, **36**, 1808.
44 R. F. W. Bader, *Atoms in molecules. A quantum theory*, Clarendon, Oxford, 1990.
45 R. Hoffmann, *Solids and surfaces: a chemist's view of bonding in extended structures*, VCH, New York, 1988.
46 J. G. Malecki, *Polyhedron*, 2010, **29**, 1973.
47 E. R. Johnson, S. Keinan, P. Mori-Sánchez, J. Contreras-García, A. J. Cohen and W. T. Yang, *J. Am. Chem. Soc.*, 2010, **132**, 6498.
48 A. Kovács and R. J. M. Konings, *J. Phys. Chem. A*, 2011, **115**, 6646.
49 W. Küchle, M. Dolg, H. Stoll and H. Preuss, *J. Chem. Phys.*, 1994, **100**, 7535.
50 D. W. Green and G. T. Reedy, *J. Chem. Phys.*, 1978, **69**, 544.
51 S. D. Conradson, *Appl. Spectrosc.*, 1998, **52**, 252A.
52 L. V. Moskaleva, A. V. Matveev, J. Dengler and N. Rösch, *Phys. Chem. Chem. Phys.*, 2006, **8**, 3767.
53 V. Bakken, J. M. Millam and H. B. Schlegel, *J. Chem. Phys.*, 1999, **111**, 8773.
54 T. Lu and F. Chen, *J. Mol. Graphics Modell.*, 2012, **38**, 314.
55 E. Di Santo, M. C. Michelini and N. Russo, *Organometallics*, 2009, **28**, 3716.
56 S. F. Vyboishchikov, A. Sierraalta and G. Frenking, *J. Comput. Chem.*, 1996, **18**, 416.
57 D. Cremer and E. Kraka, *Angew. Chem., Int. Ed. Engl.*, 1984, **23**, 627.

